

Controlled solvothermal synthesis of ultrahigh-aspect-ratio Sb_2Se_3 nanowires and their photoconductive properties

Zhe Chen · Feng Chen · Nai-Di Tan

Received: 20 August 2014 / Accepted: 6 November 2014 / Published online: 15 November 2014
© Springer Science+Business Media New York 2014

Abstract In this work, ultrahigh-aspect-ratio Sb_2Se_3 nanowires have been controllably prepared by a mild hydrothermal treatment. X-ray diffraction, X-ray photoelectron spectra, scanning electron microscopy, transmission electron microscopy, high-resolution transmission electron microscopy, and selected area electron diffraction were used to characterize the as-synthesized samples. The result revealed that the as-synthesized products were wire-like with diameter ranging from 20 to 30 nm and length of 30 μm . Meanwhile, various experimental parameters such as concentration of precursors, influence of ethylenediamine, reaction time and the formation of mechanism were discussed and properties of photoconductive of Sb_2Se_3 were also investigated in detail. In addition, to the best of our knowledge, there have been no any reports on the one-pot synthesis of Sb_2Se_3 nanomaterials under the benzyl alcohol system.

1 Introduction

Nanostructured materials, especially one-dimensional (1D) nanostructured such as nanowires, nanorods, nanobelts, and nanotubes, have been given extensive attention due to their peculiar physical and chemical properties and the wide range of potential applications in nanodevices [1–4]. In recent years, some of these materials play an important role

in optical, electrical, magnetic, and mechanical because of their different from those of bulk or nanoparticle materials. It has been reported that some 1D nanostructured materials have been employed as active components or interconnects for the fabrication of nanoscale electronic, optical, optoelectronic, electrochemical, and electromechanical devices. Especially, semiconductor nanowires are attractive subject both because of the fundamental new science that they help to uncover as well as for their potential applications in electronic and optoelectronic devices [5–7]. Therefore, synthesis of higher aspect ratio nanowires is becoming an intensive and hot research topic. As far as we know, current strategies for producing higher aspect ratio nanowires have mainly made use of the vapor liquid solid (VLS) method which often needs higher temperature, special conditions, long reaction time and complex procedures. Thereby, developing lower temperature, shorter time, inexpensive reagents, benignancy to environment and convenience synthetic process are still great challenge in the current scientific field.

Sb_2Se_3 , the main-group $\text{A}_2^{\text{III}}\text{B}_3^{\text{II}}$ metal chalcogenides (A = As, Sb, Bi; B = S, Se, Te) which have extensive applications in optoelectronic devices, infrared spectroscopy, television cameras with photoconducting targets, and thermoelectric devices, etc. [8–10]. Much more effort has been focused on the synthesis of Sb_2Se_3 nanomaterials. For example, the growth of Sb_2Se_3 nanowires also has been achieved by pulsed vapour–liquid–solid technique [11]. Sb_2Se_3 hierarchical nanomaterials have been fabricated by $\text{C}_4\text{H}_4\text{KO}_7\text{Sb}$ and NaHSe solution under hydrothermal conditions in the presence of poly (vinyl pyrrolidone) [12]. One-dimensional Sb_2Se_3 nanowires have been prepared by $\text{Sb}(\text{AcO})_3$, Na_2SeO_3 and hydrazine hydrate basic solution under hydrothermal conditions [13]. Sb_2Se_3 nanoribbons with lengths of up to hundreds of microns were obtained by

Z. Chen · N.-D. Tan (✉)
Jilin Institute of Chemical Technology, Jilin 132022, China
e-mail: jmsendt@yeah.net

F. Chen
Jilin Petrochemical Company Organic Synthetic Plants,
Jilin 132021, China

reacting SbCl_3 and Se powders in solvothermal solution for 3 days with the assistance of NaBH_4 [14]. The synthesis of Sb_2Se_3 nanorods have been carried by using alkaline selenium solution and SbCl_3 in presence of hydrazine hydrate as reducing agent under hydrothermal conditions [15]. Very recently, single-crystalline Sb_2Se_3 nanowires have been produced in the presence of reducing agent (NaBH_4) via a facile hydrothermal process [16]. However, these methods often suffer from the toxicity, high cost of organometallic precursors and special conditions, or long reaction time. In addition, most of the above investigations also used additional inorganic reducing agents, such as NaBH_4 , N_2H_4 , and so on. Thus, it is still a challenge for our researchers to seek for a simple and economically efficient route for the synthesis of well-defined Sb_2Se_3 nanomaterials.

Benzyl alcohol (BA) is an environmentally friendly high boiling solvent and has weak reducing ability which is commonly widely used in the food industry. Because of these features advantages, BA has already proven to be a suitable “soft” solvent/ligand for the synthesis of nanomaterials, such as metal oxide nanoparticles, perovskites, and hybrid materials [17–24]. However, up to now, among these synthesis products, there have been no any reports on the one-pot synthesis of Sb_2Se_3 nanomaterials under the benzyl alcohol system.

Herein, we for the first time report the synthesis of higher aspect ratio Sb_2Se_3 nanowires by a facile solvothermal route. In this paper, benzyl alcohol was used not only as a solvent but also as a reducing agent. Various experimental parameters such as concentration of precursors, influence of ethylenediamine, reaction time and the formation of mechanism were detail discussed. In addition, properties of photoconductive of Sb_2Se_3 were also investigated, which may be high potentials applied in electronic and optoelectronic devices. Such a method is expected to both academic and industrial significance.

2 Experimental section

2.1 Materials

All the chemical reagents used in this work were of analytical grade and used without further purification. SbCl_3 and ethylenediamine (en) were purchased from BeiJing Beihua Fine Chemical Reagents Company, Ltd; selenium powder (Se) purchased from Sinopharm Chemical Reagent Co., Ltd; benzyl alcohol was from Tianjin Fuchen Chemical Reagents Company.

2.2 Synthesis

The typical procedure is as follows: First, 0.04 mmol SbCl_3 dissolved into 20 mL of benzyl alcohol to form a

transparent solution. Second, 1.5 mL of ethylenediamine was added into the above suspension under vigorous stirring. After 30 min, 0.06 mmol Se powder was added to the SbCl_3 and ethylenediamine aqueous solution, under continuous stirring. Finally, the resulting transparent solution was transferred to a Teflon-lined stainless steel autoclave of 30.0 mL capacity, maintained at 160 °C for 24 h. After reaction under autogenous pressure and cooling to room temperature naturally, the precipitate was collected by centrifugation, washed with deionized water and absolute ethanol several times, and dried at room temperature in air.

2.3 Characterization

The resulting samples were characterized by X-ray powder diffraction (XRD; Rigaku D-max-rA XRD with Cu-K radiation). The morphology and dimension of samples were observed by field emission scanning electron microscopy (FE-SEM, JEOL 7500B) and the transmission electron microscopy (TEM, H-800). The microstructure of samples was determined using high-resolution transmission electron microscopy (HRTEM) on a JEM-2010 apparatus with an acceleration voltage of 200 kV. X-ray photoelectron spectroscopy (XPS, ESCALAB 250) was used to confirm the oxidation state of iron. The current–voltage (I–V) characteristics of an individual Sb_2Se_3 nanowire device were measured using a micromanipulator 6150 probe station and Keithley 4200 SCS semiconductor characterization system. The time responses of photodetectors to light illumination were measured by a current meter after shutting the light.

3 Results and discussion

3.1 Structural analysis and morphology characterization

The phase and crystallographic structure of the products were determined by powder X-ray diffraction (XRD). Figure 1a shows the XRD patterns of the Ultrahigh-Aspect-Ratio Sb_2Se_3 nanowires through a solvothermal route for 24 h. All of the diffraction peaks can be well indexed as an orthorhombic phase of Sb_2Se_3 and match very well with the standard card (JCPDS 15-0861). The XRD pattern shows that the product is devoid of any detectable impurities such as Se or Sb_2O_3 , indicating that the obtained products consist of pure orthorhombic type Sb_2Se_3 by this solvothermal method. To further confirm the composition of the nanowires, the surface analysis of the nanowires was carried out by using X-ray photoelectron spectroscopy (XPS), as shown in Fig. 2. The XPS data were collected in the constant analyzer energy mode at

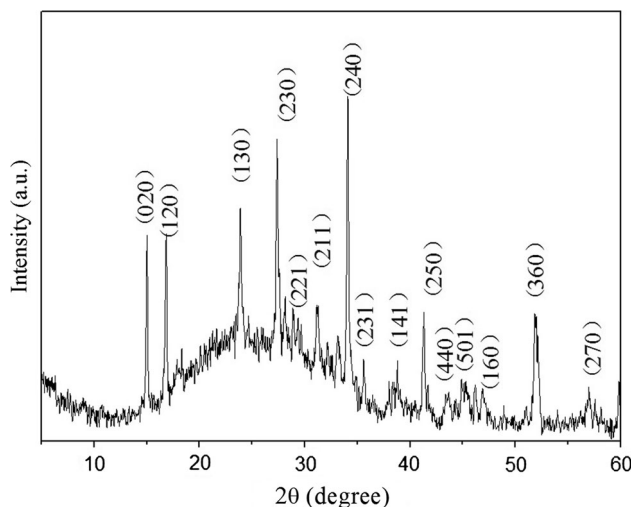


Fig. 1 XRD patterns of the as-prepared Sb_2Se_3 nanowires

20 eV. $\text{MgK}\alpha$ ($h\nu = 1,253.6$ eV) radiation was employed as the excitation source with an anode voltage of 15 kV and an emission current of 20 mA. Figure 2a, b present the XPS spectrum of Sb and Se element on the surface of the sample. The two strong peaks at 532.6 and 55.5 eV can be attributed to bonding energies of Sb3d and Se3d, respectively, which is in agreement with previously reported values for Sb_2Se_3 [25]. Thus the XPS analysis further confirms the high purity for Sb_2Se_3 sample.

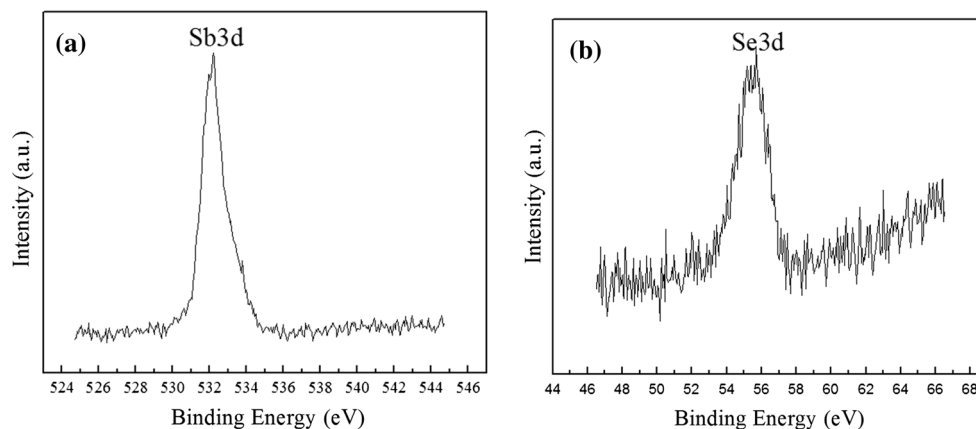
The morphology of the as-synthesized sample was investigated by field-emission scanning electron microscopy (FE-SEM). Figure 3 shows the typical FE-SEM image of the product obtained with the molar ratio of SbCl_3 to Se powder of 2:3 and the volume of ethylenediamine was 1.5 mL. As shown in the low-magnification FE-SEM image (Fig. 3a), the sample is mainly composed of a large number of uniform 1D nanowires with lengths in the range of several tens to hundreds of micrometers. No other morphologies are observed, indicating a high yield of these

samples. The high-magnification FE-SEM image in Fig. 3b revealed that the nanowires were very straight and more uniform in diameter. Further insight into the morphology and structure of the Sb_2Se_3 nanowires was gained using TEM and HRTEM. The structure was further confirmed by a low transmission electron microscopy (TEM) image (Fig. 3c), in which the uniform of diameter of nanowires can clearly be seen. One single nanowire of diameter around 25 nm and length of 30 μm has been focused and is shown in Fig. 3d, which is consistent with the SEM image in width and length of nanowires. Thus above-mentioned SEM and TEM result clearly demonstrate that Sb_2Se_3 nanowires have successfully been fabricated with diameter ranging from 20 to 30 nm and length of 30 μm . A high-resolution TEM (HRTEM) image (Fig. 3e) taken on an individual nanowire displays clear crystal lattices with d-spacing of 0.794 nm. In addition, crystallinity of these nanowires was confirmed by select area electron diffraction (SAED; inset in Fig. 3f). From this regular and clear rectangular diffraction spot array, it can be seen that the nanowire is single-crystalline structure.

3.2 Influence of different volume of ethylenediamine

To further study the influence of ethylenediamine factors on the morphology of as-synthesized Sb_2Se_3 , controllable experiments were performed by changing reaction parameters. It is found that the different volume of ethylenediamine plays an important role in the formation of uniform nanowires. Figure 4 shows the TEM image of the sample synthesized with the different volume of ethylenediamine from 0 to 4 mL while other reaction parameters are the same. If no ethylenediamine was added in the reaction system, large numbers of size and length irregular nanowires and little particles coexist in the sample (Fig. 4a). When 0.5 mL of the above ethylenediamine aqueous solution was used, these nanowires became narrower and longer but we also can occasionally see some small amount

Fig. 2 X-ray photoelectron spectra (XPS): **a** Sb 3d; **b** Se 3d



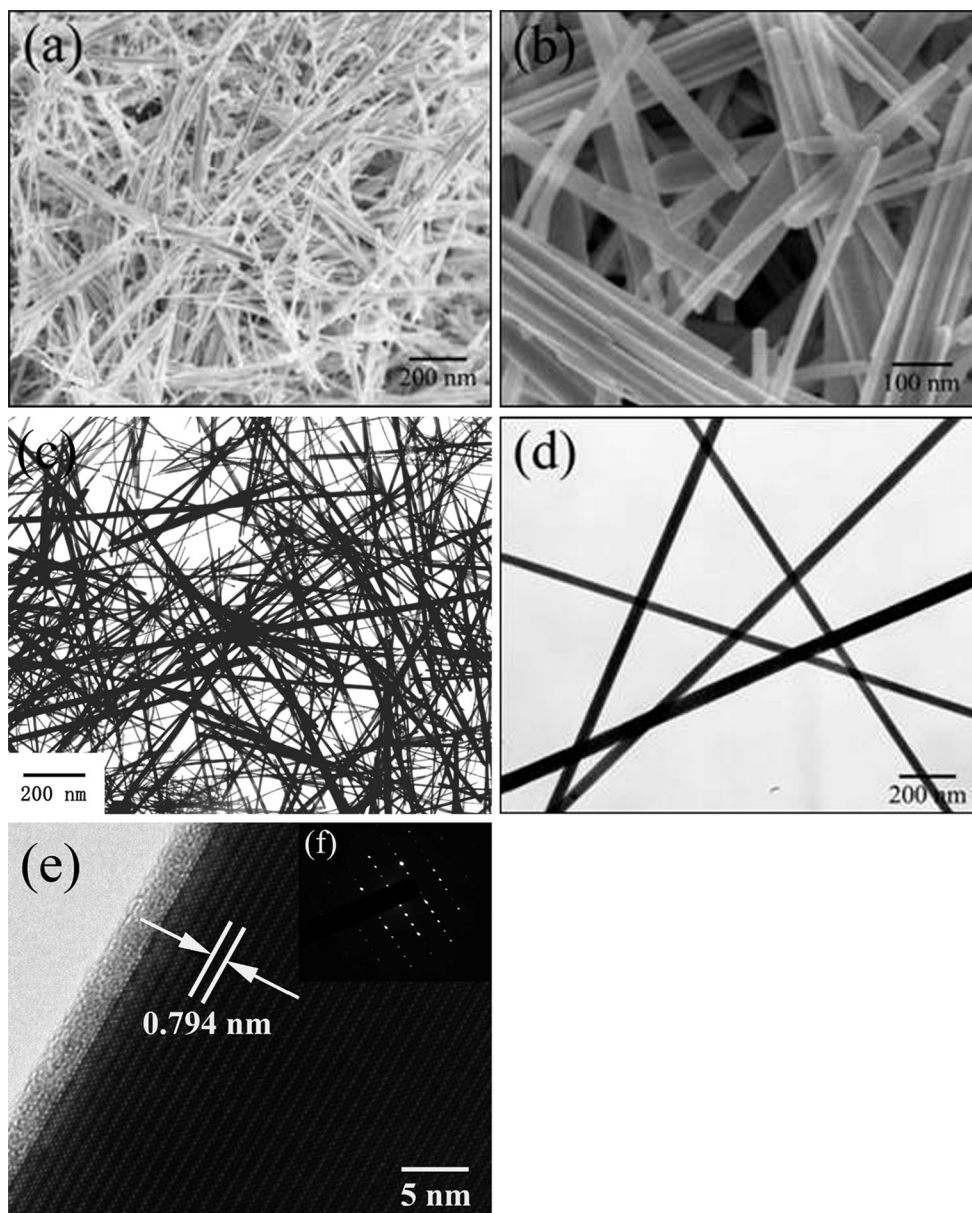


Fig. 3 Typical SEM images: **a** low-magnification; **b** an individual wire-like Sb_2Se_3 nanostructures. **c** Low- and **d** high-magnification TEM images. **e** HRTEM image of an individual nanowire. **f** SAED pattern

of particles (Fig. 4b). When 1.5 mL of ethylenediamine was used, namely the optimum synthesis condition, uniform and long nanowires were formed (Fig. 4c). With the increase of the ethylenediamine volume added (2.5 and 4 mL), the length and width of nanowires became irregular (Fig. 4d, e). When excessive ethylenediamine was used, nanowires not only became more irregular, but also aggregate together. Therefore, on the basis of above experimental results and analysis, we speculated that lower and higher of concentration ethylenediamine is not conformed uniform nanowires. When in the absence or low

concentration of ethylenediamine, Sb^{3+} and ethylenediamine is not completely ligand, which results in formation different length of nanowires. However, irregular nanowires were obtained when concentration of ethylenediamine was quite high. Due to under the condition of benzyl alcohol and ethylenediamine, these can served as reducing and alkaline for reducing Se into many Se^{2-} , these Se^{2-} can rapidly reaction with $[\text{Sb}(\text{en})_3]^{3+}$ and damaged to the dynamic equilibrium. Therefore, on the basis of the above analyses, it can be found that ethylenediamine plays important roles in formation of uniform nanowires.

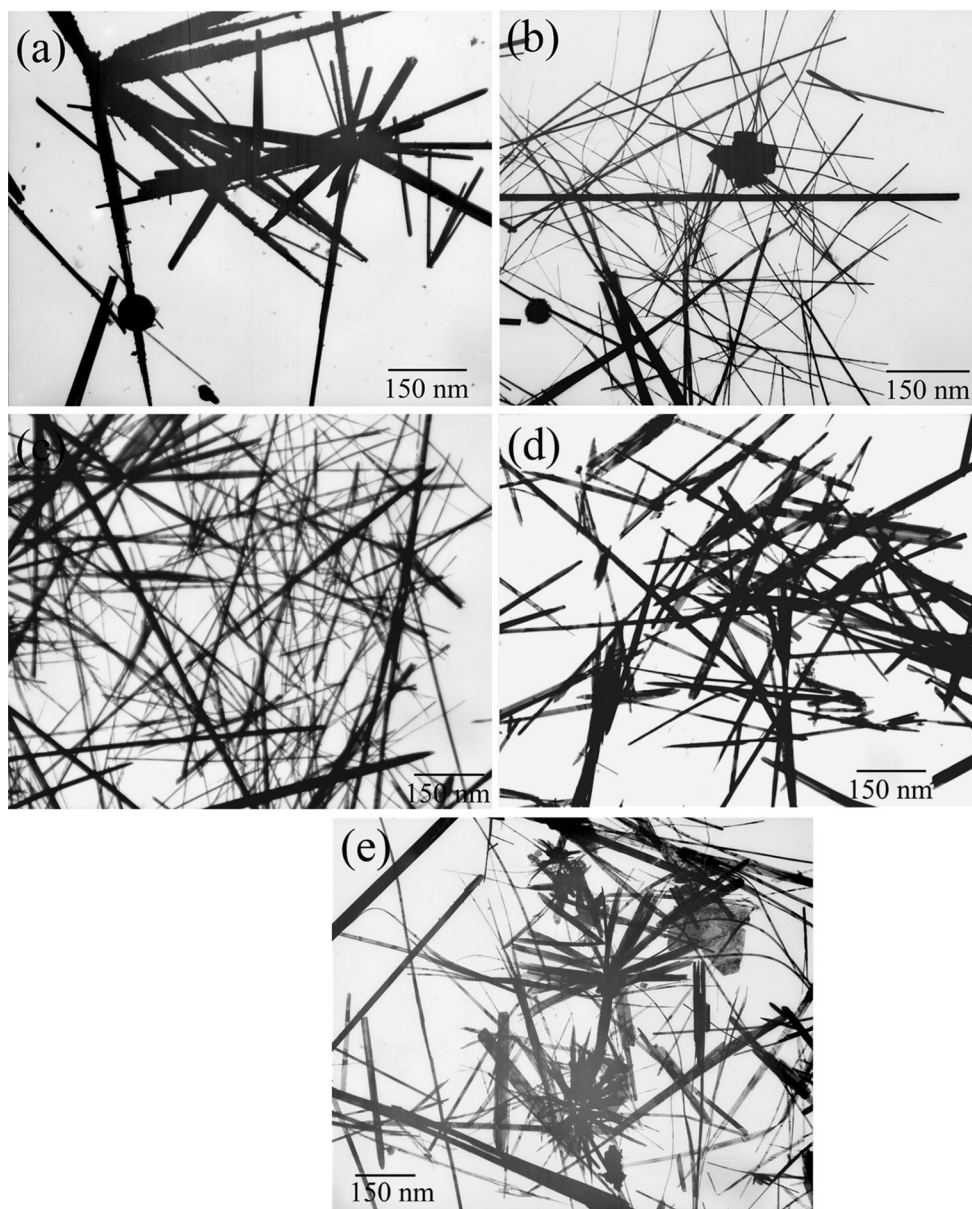


Fig. 4 TEM images of the products under adding different quantity of ethylenediamine: **a** 0 mL, **b** 0.5 mL, **c** 1.5 mL, **d** 2.5 mL, and **e** 4 mL

3.3 Influence of the concentration of precursors

To highlight the influence of the concentration of reagents, a series of experiments were carried out, as shown in Fig. 5. In our experiment, reaction with the mixed solution having different concentration of SbCl_3 of 0.02, 0.04, 0.08 and 0.16 mmol, while keeping the others fixed in the reaction system. Figure 5a indicates the TEM image of 0.02 mmol SbCl_3 , it can be clearly seen that the products are comprised of a large number of irregular and nonuniform nanowires with a different size. When 0.04 mmol of SbCl_3 was used, as shown in Fig. 5b, the perfect ultrahigh-aspect-ratio Sb_2Se_3 nanowires were obtained. When the concentration of initial

reagents was increased from 0.04 to 0.08 mmol as shown in Fig. 5c, excepting wires like structures, a few of nanoparticles were found in the product. When the amounts of SbCl_3 were increased to 0.16 mmol, numerous of nanoparticles were increased in the sample, which compared with those of Fig. 5c (Fig. 5d). Thereby, it was found from a series of experiments that the concentrations of reagents have significant effects on the morphology of Sb_2Se_3 .

3.4 Growth mechanism for Sb_2Se_3 nanowires

To understand the formation mechanism of the Sb_2Se_3 nanowires, time-dependent experiments were carried out to

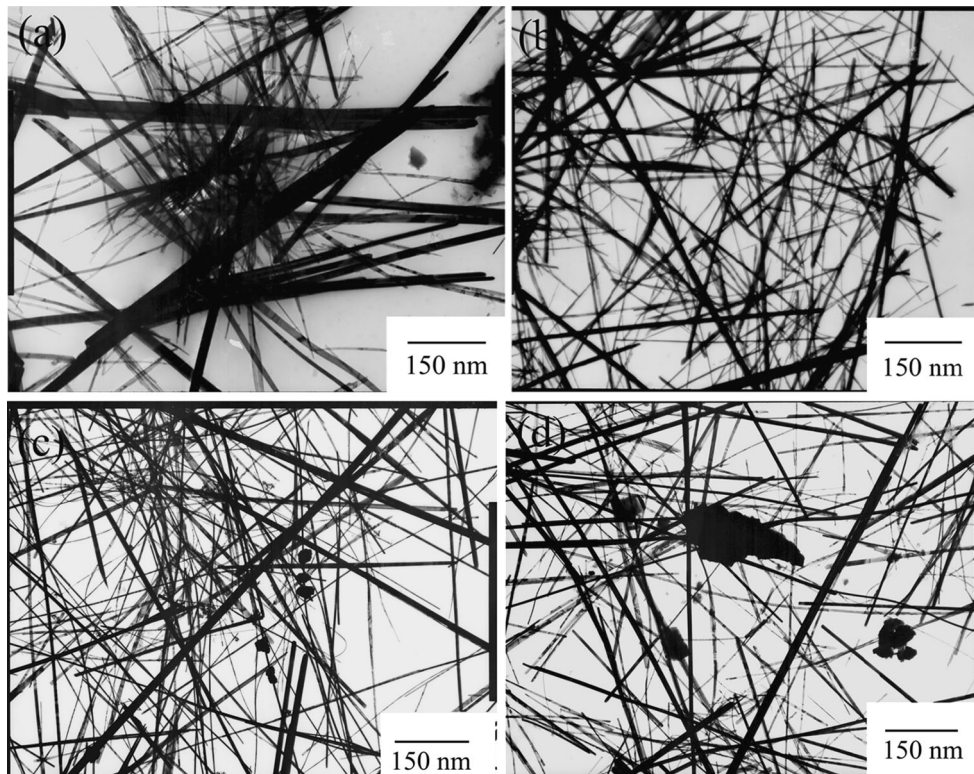


Fig. 5 TEM images of the products prepared with different concentrations of SbCl_3 **a** 0.02 mmol, **b** 0.04 mmol, **c** 0.08 mmol, **d** 0.16 mmol

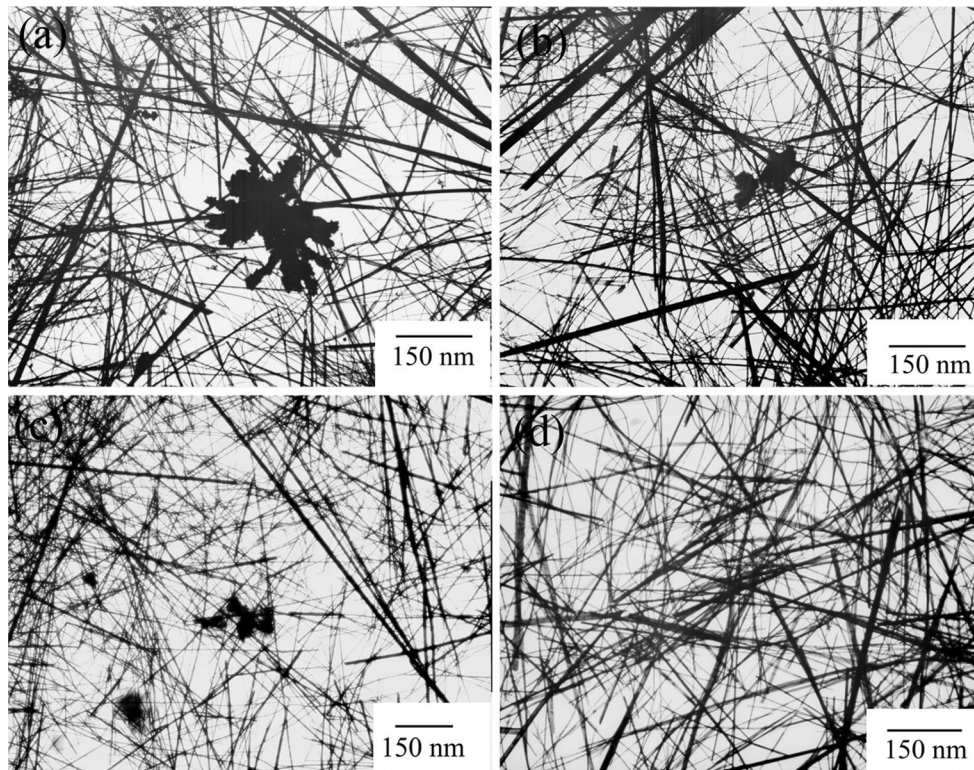


Fig. 6 TEM images of the Sb_2Se_3 nanowires obtained with different times while other experiment conditions remain the same: **a** 6 h, **b** 12 h, **c** 18 h, **d** 24 h

reveal the whole evolution process of the nanowires. As shown in Fig. 6a, it is easy to find that the sample was composed of nanowires and nanoparticles when the reaction time was 6 h. With increasing reaction time (12 h), the resulting sample still consists of nanowires and nanoparticles (Fig. 6b). When the reaction time is prolonged to 18 h (Fig. 6c), relatively uniform nanowires were formed and nanoparticles completely disappeared. And until increasing reaction time to 24 h, uniform and well-defined nanowires were finally formed as shown in Fig. 6d. Although the exact formation mechanism of these nanostructures is still unclear at present, on the basis of the TEM investigations, we propose a mechanism for the formation of ultrahigh-aspect-ratio Sb_2Se_3 nanowires. Firstly, because of N-chelation and special structure of EDA, it can easily chelate Sb^{3+} to form a relatively stable complex $[\text{Sb}(\text{en})_3]^{3+}$. Secondly, Se^{2-} was produced from the reduction of Se powder by hot benzyl alcohol. Then, tiny Sb_2Se_3 crystal nuclei formed through homogeneous nucleation. Further growth of time, these Sb_2Se_3 crystal nuclei rapidly aggregate into irregular particles and nanowires driven by the minimization of the total energy of the system via Oswald ripening process [26–28]. However, with the increase of the reaction time, the ethylenediamine existing in the solution began to corrode the irregular particles, irregular particles and nanowires and finally to form uniform nanowires by oriented aggregate. When the reaction was prolonged, the corrosion further increased, resulting in the formation of perfect uniform ultrahigh-aspect-ratio Sb_2Se_3 nanowires. Thereby, from the experimental results we know that, the two basic processes to some extent assisted each other in the formation of final stable Sb_2Se_3 nanowires in this work.

3.5 Photoconductive properties

To measure the conductivity of the products, the photoconductive properties of Sb_2Se_3 nanowires were performed and the results are shown in Fig. 7. The conductivity was measured in a dark or under illumination by using an incandescence lamp and the distance of the device-to-light source was 5 cm. The typical I–V curves of a single Sb_2Se_3 nanowire were measured in the dark or under incandescence lamp illumination (3.85 mW cm^{-2}) and as shown in Fig. 7a. In the dark, conductivity of the Sb_2Se_3 nanowires was very low, however, the conductivity of the Sb_2Se_3 nanowires dramatically increased and enhanced by 10 times compared to measurement in dark conditions, indicating that they are excellent candidates for optoelectronic switch, namely, with the dark insulating state as “off” and under incandescence lamp illuminating state as “on”. The results imply that the Sb_2Se_3 nanowires can be reversibly switched between the low and the high

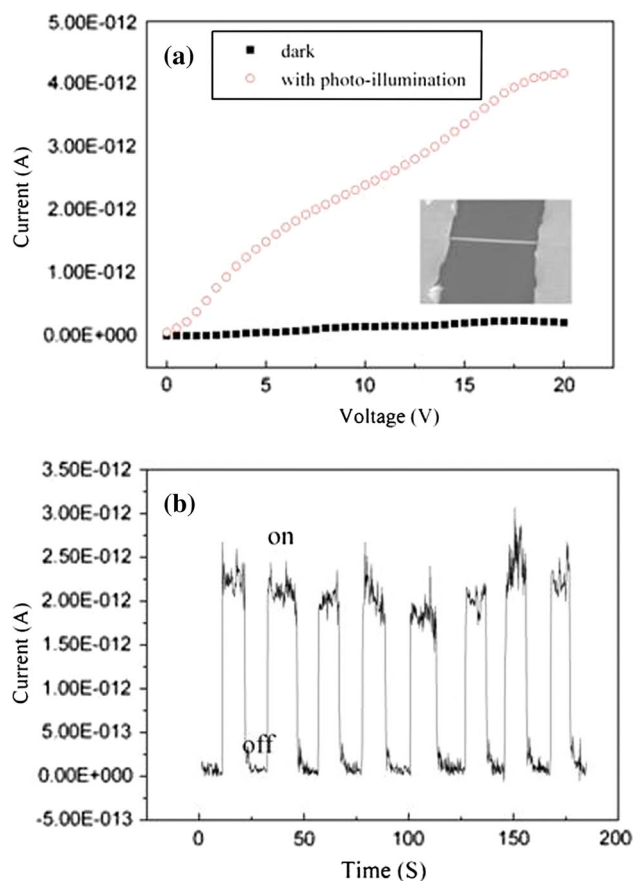


Fig. 7 Photoconductive properties of Sb_2Se_3 nanowires: **a** I–V curves of an individual Sb_2Se_3 nanowire in the dark conditions and incandescence lamp illumination (3.85 mW cm^{-2}), respectively. **b** Time-dependent photocurrent response of the Sb_2Se_3 nanowire during the light alternatively on and off at 20 s intervals

conductivity state. To further investigate the photoconductive characteristics of the Sb_2Se_3 nanowires, the time response of the product photodetector is presented in Fig. 7b. It is clearly observed that the device has a good photocurrent reproducibility and stability. The rise and decay time of conductance change were about 20 s intervals, which were shorter than many previous reports [29–31]. All these results imply that the Sb_2Se_3 nanowires are promising candidates for applications in photoswitch nanodevices.

4 Conclusion

In summary, high purity Sb_2Se_3 nanowires have been successfully synthesized by the benzyl alcohol system with the assistance of ethylenediamine. In the synthesis process, compared with the traditionally multi-step methods, we have exploited a simple and economically efficient one-pot route to synthesize large-scale, well-defined Sb_2Se_3 nanowires without the addition of any inorganic reducing agents, such as NaBH_4 , N_2H_4 , and so on. Furthermore, it is an

important point that benzyl alcohol is used not only as a solvent, but also as a reductant. In addition, a reasonable formation mechanism is proposed on the basis of the results of time-dependent experiments. Finally, the photoconductive properties of Sb_2Se_3 nanowires were investigated and the results showed this nanomaterial have good photoconductive properties. Overall, our results demonstrate the promise of these novel nanostructures as nanoscale building blocks with potential applications in high-speed photodetectors and photoelectronic switches. This synthesis strategy may open new avenues toward the preparation of other semiconductor materials.

References

1. A.I. Hochbaum, P.D. Yang, *Chem. Rev.* **110**, 527 (2010)
2. D.T. Schoen, A.P. Schoen, L.B. Hu, H.S. Kim, S.C. Heilshorn, Y. Cui, *Nano Lett.* **10**, 3628 (2010)
3. T.Y. Zhai, H.M. Liu, H.Q. Li, X.S. Fang, M.Y. Liao, L. Li, H.S. Zhou, Y. Koide, Y. Bando, D. Goberg, *Adv. Mater.* **22**, 2547 (2010)
4. T. Zhai, L. Li, X. Wang, X.S. Fang, Y. Bando, D. Golberg, *Adv. Funct. Mater.* **20**, 4233 (2010)
5. Y. Huang, X. Duan, Y. Cui, L. Lauhon, K.H. Kim, C.M. Lieber, *Science* **294**, 1313 (2001)
6. X.M. Huang, C.A. Zorman, M. Mehregany, M.L. Roukes, *Nature* **421**, 496 (2003)
7. H.M. Huang, S. Mao, H. Feick, H.Q. Yan, Y.Y. Wu, H. Kind, E. Weber, R. Russo, P.D. Yang, *Science* **292**, 1897 (2001)
8. N.A. Goriunova, B.T. Kolomiets, A.A. Mal'kova, *Sov. Phys. Tech. Phys.* **1**, 1583 (1956)
9. D. Arivouli, F.D. Gnanam, P. Ramasamy, *J. Mater. Sci. Lett.* **7**, 711 (1988)
10. T.W. Case, *Phys. Rev.* **9**, 305 (1917)
11. R.B. Yang, J. Bachmann, M. Reiche, J.W. Gerlach, U. Gösele, K. Nielsch, *Chem. Mater.* **21**, 2586 (2009)
12. Y. Guang, B.D. Chen, B.C. Guo, T.K. Zhang, W.F. Dong, W.X. Zhang, A.W. Xu, *J. Phys. Chem. C* **112**, 672 (2008)
13. J.M. Ma, Y.P. Wang, Y.J. Wang, Q. Chen, J.B. Lian, W.J. Zheng, *J. Phys. Chem. C* **113**, 13588 (2009)
14. Y. Yu, R.H. Wang, Q. Chen, L.M. Peng, *J. Phys. Chem. B* **110**, 13415 (2006)
15. O. Jyotirajan, K.S. Suneel, *Opt. Mater.* **32**, 1488 (2010)
16. T.Y. Zhai, M.F. Ye, L. Li, X.S. Fang, M.Y. Liao, Y.F. Li, Y.S. Koide, Y.S. Bando, D. Golberg, *Adv. Mater.* **22**, 4530 (2010)
17. N. Pinna, G. Neri, M. Antonietti, M. Niederberger, *Angew. Chem. Int. Ed.* **43**, 4345 (2004)
18. M. Niederberger, *Acc. Chem. Res.* **40**, 793 (2007)
19. M. Niederberger, N. Pinna, J. Polleux, M. Antonietti, *Angew. Chem. Int. Ed.* **43**, 2273 (2004)
20. M. Niederberger, G. Garnweitner, F. Krumeich, R. Nesper, H. Colfen, M. Antonietti, *Chem. Mater.* **16**, 1202 (2004)
21. N. Pinna, M. Antonietti, M. Niederberger, *Colloids Surf. A* **250**, 211 (2004)
22. N. Pinna, G. Garnweitner, M. Antonietti, M. Niederberger, *Adv. Mater.* **16**, 2196 (2004)
23. N. Pinna, G. Garnweitner, P. Beato, M. Niederberger, M. Antonietti, *Small* **1**, 112 (2005)
24. M. Niederberger, G. Garnweitner, N. Pinna, M. Antonietti, *J. Am. Chem. Soc.* **126**, 9120 (2004)
25. D.B. Wang, D.B. Yu, M.S. Mo, X.M. Liu, Y.T. Qian, J. Crys. Growth. **253**, 445 (2003)
26. B. Li, G. Rong, Y. Xie, L. Huang, C. Feng, *Inorg. Chem.* **45**, 6404 (2006)
27. W.Z. Ostwald, *Phys. Chem.* **34**, 495 (1900)
28. S.J. Bao, Q.L. Bao, C.M. Li, T.P. Chen, C.Q. Sun, Z.L. Dong, Y. Gan, *Small* **3**, 1174 (2007)
29. T.Y. Zhai, X.S. Fang, M.Y. Liao, X.J. Xu, H.B. Zeng, Y. Bando, D. Golberg, *Sensors* **9**, 6504 (2009)
30. Y.L. Chueh, C.H. Hsieh, M.T. Chang, L.J. Chou, C.S. Lao, J.H. Song, J.Y. Gan, Z.L. Wang, *Adv. Mater.* **19**, 143 (2007)
31. X. Fan, X.M. Meng, X.H. Zhang, M.L. Zhang, J.S. Jie, W.J. Zhang, C.S. Lee, S.T. Lee, *J. Phys. Chem. C* **113**, 834 (2009)